Published in final edited form as:
Nanotechnology. 2010 July 2; 21(26): 262001. doi:10.1088/0957-4484/21/26/262001.

Recognition Tunneling

Stuart Lindsay[1,2,3], **Jin He**[1], **Otto Sankey**[2], **Prokop Hapala**[4], **Pavel Jelinek**[4], **Peiming Zhang**[1], **Shuai Chang**[1,2], and **Shuo Huang**[1,2]

[1]Biodesign Institute, Arizona State University, Tempe, AZ 85287, USA

[2]Department of Physics, Arizona State University, Tempe, AZ 85287, USA

[3]Department of Chemistry and Biochemistry, Arizona State University, Tempe, AZ 85287, USA

[4]Institute of Physics, Academy of Sciences of the Czech Republic, Cukrovarnická 10, 1862 53, Prague, Czech Republic

Abstract

Single molecules in a tunnel junction can now be interrogated reliably using chemically-functionalized electrodes. Monitoring stochastic bonding fluctuations between a ligand bound to one electrode and its target bound to a second electrode ("tethered molecule-pair" configuration) gives insight into the nature of the intermolecular bonding at a single molecule-pair level, and defines the requirements for reproducible tunneling data. Simulations show that there is an instability in the tunnel gap at large currents, and this results in a multiplicity of contacts with a corresponding spread in the measured currents. At small currents (i.e. large gaps) the gap is stable, and functionalizing a pair of electrodes with recognition reagents (the "free analyte" configuration) can generate a distinct tunneling signal when an analyte molecule is trapped in the gap. This opens up a new interface between chemistry and electronics with immediate implications for rapid sequencing of single DNA molecules.

Introduction

Reading chemical identity at the single atom or single molecule level has long been a goal of the electron tunneling community. Recognition tunneling achieves that goal, serves as a remarkable probe of chemical bonds at the single molecule level and enables a new type of single molecule electronic sensor.

Atomic identification of sites on clean semiconductor surfaces in ultrahigh vacuum (UHV) was achieved by atomic resolution tunneling spectroscopy in the mid 1980's[1]. This approach has been extended to a number of molecular systems,[2] including DNA.[3, 4] Potential distributions in UHV are reproducible enough for precise molecular identification in many cases. In particular, the Hipps-Mazur lab has shown that there is a strong correlation between the bias at which features are observed in the tunneling spectroscopy and the reduction potential of the molecules.[2]

The situation is much more difficult in solution where solvent reorganization and an unknown potential distribution (owing to poorly characterized screening effects) complicate the analysis, [5] though the problem can be simplified when chemically well-defined contacts are used between the target molecules and the metal electrodes.[6, 7]

In an ingenious experiment, Tao showed that tunneling transmission could be gated by controlling the potential of a redox active molecule relative to a standard reference electrode. [8] This solves the problem of an unknown potential distribution, and single molecules can be identified, but only if they contain a redox-active species with a distinctive reduction or

oxidation feature at an accessible potential. A completely new approach was introduced by Ohshiro and Umezawa in 2006.[9] They demonstrated that STM images of molecular adsorbates showed chemical contrast if the scanning probe was functionalized with a molecule that bound to specific targets on the surface. In their work, a gold STM probe was functionalized with a thiolated DNA base, and images were made of monolayers of DNA bases, or peptide nucleic acid (PNA, a DNA analog with a peptide backbone) bonded to a gold substrate. Enhanced contrast was found when the base on the probe was the Watson-Crick hydrogen bonding complement of the bases on the substrate. Analysis of the interaction between the functionalized STM probe and the target molecules shows that it is dominated by mechanical adhesion between the probe and target molecules, with essentially no contribution by a "chemically-sensitive" tunnel current.[10] It appears that the STM probe sticks to its complementary target for a longer time as the tip is scanned, resulting in more charge transfer between probe and substrate. Thus the tunnel current serves as a method for monitoring mechanical adhesion, and the method more closely resembles friction-force chemical sensing[11] or single-molecule force spectroscopy[12] as usually implemented with an atomic force microscope. Nonetheless, a variant of the Ohshiro-Umezawa method does permit identification of molecular species on a surface[13] and has been used to "read" the composition of DNA oligomers, albeit with a resolution limited to blocks of about ten bases, owing to the strong mechanical interactions between the probe and surface.[14]

We have recently refined the method further, and it is now at the point where true single molecule reads are possible with the exquisite degree of recognition that comes from matching sets of hydrogen-bond donors and acceptors on probe and target.[15] Rather than move the probe relative to the substrate, we fix a tunnel gap and monitor the stochastic fluctuations in bonding as the target molecule binds, unbinds and rebinds the probe molecule (Figure 1A). Such stochastic switching has been observed before as a consequence of the lability of thiol contacts between a molecule and a gold surface,[16] and was used as the basis of an ingenious method for measuring single-molecule conductivity introduced by Nichols and Haiss.[17, 18] This gives rise to a characteristic "telegraph" noise in the tunnel current as illustrated in Figure 1B. The gap is set to an initial "baseline" conductance, G_{BL}, the current increasing by an amount corresponding to the "on conductance", ΔG_{ON} when a molecular bridge spans the gap. In the first implementation of "Recognition Tunneling" (which we call the "tethered molecule-pair" configuration, Figure 1A, B) we have measured the conductance of Watson-Crick base pairs using a base bonded to a probe and a nucleoside bonded to a surface, and monitoring the telegraph noise generated both by breaking of the hydrogen bonds and by breaking of the gold-thiol contacts used to hold the molecules to electrodes.[15] These measurements permit direct probing of bonds between single molecule pairs, measuring both their lifetimes and their electronic transport properties.

In a further refinement of Recognition Tunneling (which we call the "free analyte" configuration, Figure 1C), we have functionalized a pair of tunneling electrodes with molecules that present both hydrogen bond donors and acceptors, setting the gap to be large enough for target molecules to diffuse into it and bridge the sensing molecules on the surface to the sensing molecules on the probe via a network of hydrogen bonds. Differences in the pattern of hydrogen bonding lead to different levels of tunnel current as targets bind transiently in the gap (Figure 1D). These signals can be distinctive enough to allow the identity of the four DNA bases to be read with a confidence level that is greater than 0.6 on a single molecule read.[19] This technique could be adapted to read small drug molecules, metabolites, amino acids, small peptides and so on.

It is the purpose of this review to provide a simple background to Recognition Tunneling, an outline of hydrogen-bond mediated tunneling and a description of experimental methods, as well as a summary of the results obtained to date. We provide, in addition, new modeling that

we have carried out to understand the way in which the telegraph noise distribution changes with the size of the tunnel gap.

Key ideas in tunneling

We begin with a brief overview of the phenomenon of electron tunneling. Technical details are available in a number of theoretical reviews.[7, 20-24]. Figure 2A shows a pair of metal electrodes, separated by a gap, *L*. The electrons that transport current lie near the highest occupied state at the Fermi energy, E_F. The potential barrier that retains electrons within the metal is *V* volts so the work function, ϕ, is given by $\phi = V - E_F$. In the absence of a state in the gap (i.e., without the state represented by the thick line Δ*E* above the Fermi energy) the tunnel conductance is given approximately by

$$G \approx G_0 \exp\left(-1.02\sqrt{\phi}L\right) \equiv G_0 \exp\left(-\beta L\right) \quad (1)$$

where $G_0$is the quantum of conductance, $\frac{2e^2}{h}$=77.5 μS, ϕ is the work function in units of eV and *L* is the tunnel gap in Å. Thus, when an automatically-sharp point contact is made, the conductance is approximately 77.5 μS, falling by a factor of 10 for each Ångstrom that the gap is opened for a metal like gold (ϕ ≈ 5eV). This very rapid decay with distance is what makes tunneling such a localized probe and therefore capable of reading single bases in a DNA polymer.

If an electronic eigenstate exists in the gap, then the effective barrier is reduced to approximately Δ*E* (thick solid line in Figure 2A). *β*, the inverse electronic decay length is then given by $1.02\sqrt{\Delta E}$ if this state connects the left and right electrodes. A real molecule spanning the gap will consist of molecular orbitals often well described in terms of linear combinations of the atomic orbitals of the constituent atoms and the hopping matrix elements between adjacent orbitals. Figure 2B is a schematic representation of this situation showing atomic states closest to the Fermi energy (E_1 - E_4) with hopping matrix elements H_{L1}, H_{12}....H_{34}, H_{4R}. Thus, the states of the system, ψ_n, are molecular orbitals, as modified by interactions with the left (H_{L1}) and right (H_{4R}) electrodes.

Quantum mechanics requires that the probability amplitude for every path that connects the left electrode to the right electrode be added. The paths are all those for which molecular orbitals interact with both electrodes. The probability that an electron is propagated to the opposite electrode is then calculated from the square of this sum of probability amplitudes. Mathematically, the transmission is calculated with a Green's function:

$$G_{L,R}(E) \sim \sum_n \frac{\langle L|\psi_n\rangle \langle \psi_n|R\rangle}{E - E_{0n} + i\varepsilon} \quad (2)$$

Here, *L* and *R* represent states at the energy *E* on the left and right electrodes and E_{0n} is the eigenenergy of the n^{th} eigenstate of the system and ε is an infinitesimal. The overall conductance is calculated from $\frac{2e^2}{h}\int_{-eV/2}^{eV/2} T(E)\,dE$, where T is the transmission function and the integral extends over energies above and below the metal Fermi-levels by an amount equal to the applied bias “V.” The transmission function involves an (L,R) matrix element of $|U\ G\ U|^2$, where U is the “perturbation” connecting the L and R electrodes to the molecules wired between them.

Equation 2 casts the result as a two terminal Büttiker expression[25] for the current in terms of a transmission function. The means to calculating the transmission function is through the quantum mechanical Green's function. The earliest development the quantum mechanical formulations in terms of local (atomic) orbitals was constructed by Caroli et al.[26] There have been many applications of this formulation and it has been developed using a variety of local orbital techniques.

The key ingredient in all formulations is the Green's function operator, $(E - H)^{-1}$, where H is the electronic Hamiltonian. In the time domain, this operator is the time evolution operator $e^{-iHt/\hbar}$. It contains all the information concerning the coherent propagation of the electrons through the molecules. The Hamiltonian H describes the left-metal, molecule(s), right-metal and the couplings, U, between the left-metal and molecule(s) and between the right-metal and molecule(s). In its simplest form the propagation through the molecule contains elements of the Green's function of the form shown in Equation 2.

The full theory can be cast as a scattering problem – an electron comes in (say) from the left-metal, is scattered by the molecule(s) manifest by tunneling, and finally enters the right-metal. This scattering formulation treats the problem as three non-interacting systems (with net Hamiltonian H_0) and with an interaction/coupling perturbation U that connects the three systems and allows transmission. The complete system Hamiltonian H is $H_0 + U$. The coupling U is included to all orders where the interacting Greens function $G(E)=(E-H)^{-1}$ is written in terms of the non-interacting Green's functions, $G_0(E) = (E-H_0)^{-1}$. Dyson's equation relates the two, $G=G_0+G_0UG$. The scattering results in transitions from one metal to the next by a Fermi's golden rule formula where the effective perturbation is UG(E)U, rather than just U as in a textbook formula for Fermi's golden rule. This is the approach taken by Tomfohr et al.[27] where a full discussion of the theory and how it is implemented in local orbital density functional theory can be found.

The presence of G(E) in the transmission includes the energy levels of the molecule and naturally introduces the possibility of resonances and multiple reflections. Keldysh-like[28] formulations of non-equilibrium Green's functions go further in that they incorporate effects of the self-consistent shifts of the atomic orbitals that are produced by the electric field introduced by the bias.[29, 30]

The form of the Green's function (Equation 2) has some important experimental implications. If the connection is severed (U=0), the current drops to zero. The Green's function of the molecule is dressed by the contacts broadening out the electronic levels. Under most conditions, the Green's function propagator between the two contacts decays exponentially, which is a signature of electron tunneling. The key point here is that the states that mediate tunneling are those that overlap *both* the left and right electrodes. Any “break” in the quantum coupling between the electrodes will not allow the two terms in the numerator of equation 2 to be non-zero simultaneously. This has two consequences. The first is that molecules must be coupled to the electrodes, and the most robust way to do this direct chemical bonding between the ends of the molecule and the electrodes.[6] The second consequence is that the coupling strengths throughout the system (the H_{mn}) must be large enough not to be disrupted by thermal fluctuations.

The discussion that follows equation 1 appears to imply that $\beta \rightarrow 0$ as $\Delta E \rightarrow 0$ (i.e., $\phi \rightarrow 0$ in equation 1). In solid-state systems, this is one condition for resonant tunneling (the other being tight coupling to the electrodes [31]). In polarizable molecular systems the corresponding process is electrochemical reduction, the charge being trapped on an acceptor level by molecular and solvent reorganization. This is generally an undesirable outcome: Many redox processes are irreversible as a consequence of the generation of reactive species that, in turn, can alter the

readout system itself by reacting with recognition molecules. Secondly, redox processes on single molecules can be quite heterogeneous if the environment is heterogeneous.[32]

Given that redox processes are to be avoided, how close to the Fermi level can a state of the combined electrode-molecule-electrode system be? There are two ways to address this, both leading to the same answer. Acceptor states on the molecule will be distributed over a range of energies comparable to thermal energy, k_BT. Thus we require $|E - E_{0n}| > k_BT$ to avoid redox processes. However, we also require that the 'weakest link' in the system, $H_{mn}^{weakest} > k_BT$ for quantum coherence to be maintained across the gap. Since the smallest energy splitting ($2\Delta E$ if we assume the Fermi level is in the middle of the molecular gap so that the closest orbital is shifted by ΔE from the Fermi level) is approximately equal to $2H_{mn}^{weakest} = 2\Delta E$, we conclude that we require $\Delta E >> k_BT$. Thus β cannot be zero.

The foregoing discussion allows us to estimate the largest distance over which single molecule recognition tunneling reads may be made as follows: Let us require $\beta \geq \sqrt{10k_BT} \geq 0.5 \quad \text{Å}^{-1}$. Let us assume a minimum read time of 1ms and that our electronics has an input capacitance of 1 pF (it is difficult to do better than this). Then the current-to-voltage conversion resistor cannot be greater than 1 GΩ (so that RC = 1ms) so the Johnson noise (given by $i_{RMS} = \sqrt{\frac{4k_BT\Delta f}{R}}$) in a bandwidth, Δf = 1 kHz is about 0.1 pA. Assuming a maximum applied bias of 0.5 V (less than this will often be required to avoid redox processes) the smallest useful gap conductance is then 0.2 pS. According to equation 1, this corresponds to a value of βL=19.7 which, $\beta \geq 0.5$ Å^{-1} yields a maximum value for L of about 4 nm. This is the maximum possible value with energy levels in just the right place with respect to the Fermi level. In less favorable situatios, this maximum distace will be smaller. Thus Recognition Tunneling is restricted to combinations of analytes and reading reagents that are smaller than 4 nm. Taking the target to be no more than 3 nm diameter would limit the upper read size to proteins of no more than 10^4 Daltons (assuming that the electronic structure was just right).

Tunneling in hydrogen bonded systems

Hydrogen bond strengths lie between those of covalent and Van der Waal's bonds.[33] With bond strengths in solution of just a few times k_BT, hydrogen bonds make an ideal "molecular Velcro" for making transient contacts to analytes for applications like DNA sequencing. Can reasonable tunnel currents be sustained through such "weak" bonds? In fact, this is not the right way to ask the question, for the bond strength is related to the overall lowering of electronic energy in occupied states, whereas the tunneling rate will be determined by the energy difference between the Fermi energy of the metal and the state closest to it that spans the tunnel gap (c.f. equation 2). We need to determine, for a hydrogen bonded system, the β to use in equation 1.

One simple way to determine an upper limit on β is with complex band structure.[34] This technique uses standard (fast) codes for determining the band structure of a periodic system, but uses a complex wavevector, keeping track of the results for both the real and imaginary components. States with an imaginary wavevector are forbidden in truly infinite systems but are allowed for finite (e.g. molecular) systems. The magnitude of the imaginary wavevector is the inverse decay constant over 2, β/2, for that state (β/2 being a real variable in a decaying wave-function and β the decay constant for electron density). Assuming that the state that mediates tunneling at the Fermi energy lies halfway between the HOMO and the LUMO, the value of β can be read directly from the imaginary part of the complex band structure. A very simple (and chemically unrealistic) model of an H-bonded system is shown as the line of planar water molecules on the left of Figure 3A. They are arranged in an infinite lattice of lattice constant a, and the band structure calculated with local orbitals is shown to the right.[35] The

states with imaginary wavevector are plotted to the right, and the value of β midway between the HOMO and LUMO is 0.99 $Å^{-1}$ (9.9 nm^{-1}). This is very close to the value found in sigma-bonded systems like alkane chains. Thus, this hydrogen bonded system, despite being held together by "weak" hydrogen bonds, propagates electrons as well as an alkane chain. This is not a new result. Studies of optically-excited electron transfer mediated by π-bonds, hydrogen bonds and σ-bonds show that the transfer rate via hydrogen bonds is greater than that via σ-bonds.[36]

The value of 0.99 $Å^{-1}$ for β for the water chain is calculated for the whole system comprising a unit cell of the lattice in an infinite chain (Figure 3A). When the β strictly associated with the H-bond itself is calculated from the conductance decay as just the hydrogen bonds are stretched, a much larger value (of about 3 $Å^{-1}$) is calculated.[35] Thus the current should be very sensitive to straining of these bonds.

In reality, the Fermi level alignment is rarely exactly halfway between the HOMO and LUMO. Exact Green's function calculations are required for the entire molecular system as connected to semi-infinite slab electrodes. Structures for the two Watson-Crick base pairs, a G:T "wobble" base pair and a triply-bonded 2-aminoadenine:thymine base pair are shown in Figure 3B. The yellow atoms are the sulfur atoms that were place in a three-fold hollow on Au(111) surfaces (all structures were relaxed prior to calculation of the Green's function).[37] The calculated density of states for each type of atom (color coded as explained in the Figure caption) is shown in Figure 3C. The solid lines are projected for atoms in the purines and the dashed lines are for atoms in the pyrimidines. The Fermi level lies close to the LUMO where states are dominated by the pyrimidines. In consequence, the effective β for these molecular systems is quite small and the calculated tunnel conductances quite high.[37]

Probing single molecule junctions with telegraph noise

Haiss and Nichols pioneered the monitoring of stochastic fluctuations in molecular junctions as a method for determining the single molecule conductance.[17,18] In this technique, a molecule with two reactive end groups (thiols) is trapped between two (gold) electrodes. Stochastic fluctuations of the metal-molecule interface[16] result in a train of "on"-"off" switching events in the tunnel current (Figure 1B). If a single molecule is trapped, then this current has just two levels ("on" and "off") and so resembles the telegrapher's Morse code, hence "telegraph noise". Surprisingly, this method has not been widely adopted yet. It has some advantages over the more popular "break junction" methods.[38, 39] Firstly, the signal identifies junctions containing single molecules unambiguously because switching of more than one molecule gives rise to more than two levels in the current. In the case of break junction data, the number of molecules in the tunnel gap has to be inferred statistically. Secondly, the junction remains static, avoiding the constant reforming that occurs with break junctions. And finally, because of the separation of the two electrodes, it is possible to study different molecules on the probe and substrate, desirable for the "tethered molecule-pair" version of Recognition Tunneling. These would be rapidly scrambled in a break junction measurement.

Haiss and Nichols reported that the molecular conductances measured with telegraph noise varies with the gap, and can become multivalued at small gaps. [17, 18] For these reasons, we have found it convenient to make a scatter plot of ΔG_{ON} vs. G_{BL} and data for three combinations of basepairing have been presented in this form elsewhere. [15] We have now measured several other types of molecular junction (Chang et al., unpublished) and use some of this data here to show what appear to be rather universal characteristics. Figure 4 shows data for a guanine-cytidine junction (A) and a junction spanned by just an octanedithiol (B). The guanine-cytidine junction data are representative of the two other base-paired systems studied to date. [15] In all these systems, there is a region where ΔG_{ON} increases approximately linearly with G_{BL} (i.e.,

exponentially with decreasing gap) at very small conductances (i.e., large gaps) as shown by the region enclosed by the green box on the lower left corners of Figs. 3A and 3B. As G_{BL} is made larger, measured values of ΔG_{ON} spread out over an increasing range of values between a lower "constant" plateau (red dashed boxes) and an upper bound that increase with G_{BL}. Understanding this behavior is critical for the design of Recognition Tunneling readers.

What is going on in these junctions?

We have simulated a junction containing octanedithiol, using the calculated interaction forces in the junctions to predict the types of structure that are likely to arise as the molecule and electrodes influence each other. As we show below, gaps of different sizes are spanned by configurations that involve distortions of both the molecular bonds and the bonds in the metal contact, as well as the molecule-metal bond. We then calculated the electronic conductance for a number of these optimized structures.

Total energy DFT calculations were carried out using the VASP code,[40] within generalized gradient approximation PW91[41]. We have studied the system consisting of a single octanedithiol molecule sandwiched between two gold electrodes represented by two asymmetric surfaces having a~(3×3) periodicity in the xy-plane. We also imposed periodic boundary conditions in the direction perpendicular to the surface, artificially joining the last two layers of the system. The stretching of the system is simulated by increasing the distance between the two limiting layers by steps of 0.25Å. After each step, the system was allowed to relax toward its configuration of minimum energy; in this relaxation, only the atoms located in the last two layers remain fixed. The convergence criteria for total energy and force were 10^{-6} eV and 10^{-2} eV/Å, respectively. Plane-wave functions were expanded on a mesh of 12 Monkhorst-Pack (MP) k-points on the two-dimensional Brillouin zone with a plane-wave cutoff of 290 eV.

Subsequently, we used the optimized atomic structures to calculate the current flowing through molecular junctions. The conductance calculations were carried out using the Green's function formalism[42] implemented in a local basis set DFT code (Fireball[43, 44]) using 64 MP k-points. The results of these simulations are shown in Figure 4C.

The calculated conductances are about an order of magnitude higher than the measured conductances but the general shape of the ΔG_{ON} vs. G_{BL} simulated plot (Figure 4C) is strikingly similar to the measured data (Figure 4B): (1) At low values of G_{BL} the simulated data shows a region where ΔG_{ON} increases linearly with G_{BL}. (2) Above a threshold value of G_{BL}, data for ΔG_{ON} is multivalued, with the maximum value rising with increasing G_{BL} at about he rate observed in the experimental data.

The simulations were carried out for number of contact geometries, only a representative selection of which (A-D) are presented here with their structures illustrated in Figure 5. An important result is that the tunneling current is insensitive to contact geometries at the largest gaps. Figure 4C also plots the "vacuum gap", Z_{VAC} between the gold atom attached to the molecule and the remainder of the gold cluster (Figure 5E). The region of monotonic dependence of ΔG_{ON} vs. G_{BL} corresponds to the "non-contact" region where Z_{VAC}varies rapidly with G_{BL} Figure 5E shows an example of how contact geometry can vary spontaneously over the course of repeated making the breaking of contacts: the lower contact reorganizes on breaking of the top contact. Note how this simulation (and others like it) show clearly that it is an Au-Au bond that breaks and not an Au-sulfur bond. This result is predicted on the (usually-assumed) dissociative adsorption of SH on Au, but there is some evidence the hydrogen remains on the surface.[45] The same picture is recapitulated in our simulations of non-dissociative adsorption, save that it is the SH-Au bond that is the weak link that stretches (as opposed to

the (Au-S)-S bond), however the (Au-S)-S bond is found to be more stable than the (Au-H)-S bond by about 1 eV in our calculations.

This region of monotonic ΔG_{ON} vs. G_{BL} ("non-contact") sensing may require a flexible molecular junction, for such a region is absent in data obtained with a stiff molecule (dibenzenedithiol -Figure 4D). The DFT calculations capture this behavior for this molecule too. The molecule jumps directly from a non-bonded to a bonded configuration with no intermediate stretching (Hapala and Jelinik, in preparation).

Finally, this analysis suggests that an "equilibrium" configuration occurs just when a molecule first jumps into contact. In a probe of finite radius, we expect that many such configurations arise, and that these correspond to the "plateaus" observed in the plots of ΔG_{ON} vs. G_{BL} (red dashed boxes in Figures 4A and 4B). For DNA base-pairs, the average values of conductance obtained from these plateaus lie within a factor two of the predicted values, and follow the theoretically-predicted order of conductances.[15]

Bond breaking, bond fluctuations and telegraph noise

Here, we want to draw a distinction between "electronic bond breaking" (i.e., shutting off tunnel transport) and "mechanical bond breaking (i.e., completely separating the bonding partners). The first observation of these bonding fluctuations by scanning tunneling microscopy [16] showed that the conductance fluctuated while the molecule remained in place. This implies that small fluctuations in bonding can disrupt the electronic coupling essential for tunneling while leaving the molecule still "attached" to the surface. Despite this caveat, the distributions of "on" times clearly contain chemical information, as shown in Figure 6. Figure 6A shows distributions (left sides of the panels) for guanine interacting with cytosine (G:C), 2-aminoadenine interacting with thymine (2AA:T) and adenine interacting with thymine (A:T – structures are shown in Figure 6B). The lifetime distributions are clearly bimodal, with one peak near 45 ms (S-Au) and another near 8 ms (HB). Contrasting these distributions to that measured for an octanedithiol (Figure 6C) shows that the 45 ms features are a consequence of fluctuations of the (S-Au)-Au bonds, so that the 8 ms features must be associated with the hydrogen bonded complexes. The differences in lifetime between the two- and three-hydrogen bonded complexes is small (and the distributions are very wide) but the relative frequency of hydrogen bond breaking is clearly larger relative to (S-Au)-S breaking in the A:T complex than in the G:C and 2AA:T complexes.

The lifetime histograms are resolved as a function of G_{BL} on the right-hand side of Figure 6A. Interestingly, there is little evidence of (S-Au)-Au bond breaking at small G_{BL} in the "non-contact" region. Hydrogen bond breaking dominates initially, but then falls off rapidly with increasing G_{BL} . At small gaps (S-Au)-Au bond breaking appears to be the dominant mode, possibly because of the fact that (S-Au)-Au bond is an intrinsic property of the Au surface. In contrast, the hydrogen bonded components appear to require space to accommodate fluctuations. The intrinsic lifetime of these bonds in a confined space may be very long.

These data clearly demonstrate the ability of this technique to extract bonding information on a single molecule basis. Recent (unpublished) studies of the bonding lifetimes that use force spectroscopy to estimate the off-rate in nanojunctions suggest that the true off rate is very slow. If this is indeed that case, then the system remains "bonded" for long times, with the telegraph noise reporting local fluctuations that interrupt tunnel current, consistent with what was observed by scanning tunneling microscopy.[16] The exact nature of these fluctuations is unknown, but it is clear that tunneling will report on even small (atomic-scale) disruptions of the bonding. For example, a motion of just 1 Å will reduce current by a factor 20x.[35] On the other hand, the long range electrostatic interactions between charged sites will still contribute significantly to bond strength at much larger separations. Therefore, it is possible for the tunnel

current to drop below the background noise while a significant bonding energy remains. This could explain one of the experimental mysteries of Recognition Tunneling. The stability of the tunnel junctions is quite remarkable even in the absence of servo control, currents remaining stable for periods of up to ten seconds. Perhaps the junctions are held together by bonds that are stable on time scales that are much longer than the timescale of the telegraph noise fluctuations.

Recognition Tunneling for detection of single molecule analytes

The foregoing discussion of the "tethered molecule-pair" configuration (Figure 1A) sets the stage for design of a new type of analytical system that traps analytes, the "free analyte" configuration, illustrated in Figure 1B. We recently implemented such a scheme for recognition of DNA nucleosides[19] using 4-mercapto benzoic acid as the recognition molecule (here R1=R2 in Figure 1C). In organic solvent (trichlorobenzene) the benzoic acid is neutral, containing a hydrogen bond donor and a hydrogen bond acceptor. Pairs of this reagent can form four distinctive hydrogen bonded complexes with all four DNA bases as shown in Figure 7 A-D. [19] The choice of gap size is critical. Any larger, and the smaller bases (like T) will not be trapped on both sides. On the other hand, smaller gaps offer the possibility of multiple binding arrangements for larger bases (like A). At this large gap value (2.5 nm, calculated from measured tunnel decay rates[13]) the background tunnel current is just 6 pA (at a bias of 0.5V) so that the small gap conductance (12 pS) ensures that we are in the "non-contact" regime where contact geometry variations in conductance appear to be insignificant. In the absence of analyte, the signal (Figure 1E) is also free of the noise spikes that occur in smaller junctions where the benzoic acids molecules can bond with each other across the junction. When nucleosides are injected into the solvent that surrounds the tunnel junction, current spikes are seen almost immediately (Figure 1F). These events often show the telegraph noise (inset) characteristic of binding and unbinding events. This particular reading reagent gives distinctive current reads for each of the four bases, and experimentally measured current distributions are shown in Figure 7G. Reads are not completely separated, but the overlap is such that a correct assignment can be made at the 0.6 confidence level (or better) on the first read. We have also shown that mixtures of bases give clearly resolved signals.[19]

It is instructive to probe the role of the recognition reagents by comparing reads with, and without them. Figure 8A shows a distribution of currents measured in a somewhat smaller gap (baseline conductance = 20 pS) with a bare gold substrate and probe. The target is deoxyguanosine (the gap had to be decreased somewhat in order to observe current spikes with no functional groups on the electrodes). When one electrode in the gap is functionalized (and set to a baseline conductance of 12 pS) the resultant distribution is dramatically narrowed (Figure 8B). A second small peak at twice the current of the first peak appears, a characteristic feature of junctions like this when two molecule span the gap.[7] Functionalizing both electrodes does not decrease the width of the distribution any further. It appears that the target is trapped by the hydrogen bonds, eliminating motional broadening of the tunnel current distribution, but this is not the correct interpretation of the narrowing. This can be seen from the measured distributions of on-state lifetimes shown in Figure 8C. The distributions are very similar for bare electrodes (blue line) and one functionalized electrode (red). Thus the trapping time of molecules in the gap does not depend strongly on the chemical functionalization of the gap. Similar results were obtained for the other three bases.[19] It is known that the bases interact quite strongly with gold via the lone-pair electrons on the imines and amines, so the reads taken with bare electrodes almost certainly reflect transient binding of the targets to the gold electrodes. Thus the observed narrowing of the current distribution on functionalizing one of the electrodes reflects a reduction in the range of *static* bound conformations. Tunneling reads require an interaction between the target molecules and the electrodes. Recognition Tunneling makes this a controlled interaction.

The future

Clearly, Recognition Tunneling is a powerful new tool for investigating bonding in a small junction. It is clearly capable of single molecule detection and might enable a new class of single molecule sensors. As far as DNA sequencing goes, three questions remain: (1) Can the bases be distinguished with reads made in aqueous buffered electrolyte? (2) Can single base resolution be obtained in the context of a DNA molecule where each base is separated by about 0.3 nm? (3) Can chemical modifications of the bases (important as epigenetic coding) be read? Preliminary work in our laboratory suggests that the answer to all three questions is positive. Electrochemical leakage in aqueous buffer is not a problem with good insulation[46] of tunneling probes. Signal levels appear to be even larger that those found in organic solvent, despite the expectation that hydrogen bonding between the recognition elements will be weaker in water because of competition from water molecules.

Evidence for single base reads is seen in long runs of telegraph noise as small DNA oligomers with an alternating base sequence are trapped in the gap (Huang, manuscript in preparation). If more than one type of base contributed to the signal, this two level switching would be hard to account for. Finally, experiments with deoxycytidinemonophosphate and 5-methylcytidine monophosphate show that there are clear differences in the size of the tunneling signals. It appears that hydration is playing a role here, because no difference was observed between deoxycytidine and 5-methyl-deoxycytidine measured in organic solvent.[19] Methylation has long been known to affect the melting temperature of double helical DNA, reflecting its effects on the bonding between helices in water.[47]

Recognition tunneling is not limited to nucleic acid targets (DNA and RNA). Half of the amino acid residues have hydrogen-bonding sites in addition to those on the peptide backbone itself. Five (asn, glu, gln, his, arg) have at least two or more sites while another five (lys, ser, thr, try, trp) have one other site available. This raises the possibility of identifying specific peptide sequences in protein biomarkers using Recognition Tunneling, thus avoiding immunoassays that require antibodies for recognition and detection.

Acknowledgments

We acknowledge financial support from the DNA sequencing technology program of the National Institute of Human Genome Research (HG004378).

Appendix

Experimental Methods

A Characterization of molecule layer on metal surface

Molecule monolayers were formed by adsorption of thiolated molecules onto flame-annealed Au(111) substrates.[48] STM imaging showed that 5'-thiolated-nucleosides normally form disordered monolayers. The thickness of the adlayers was measured by ellipsometry and found to be consistent with a monolayer. Fourier transform infrared spectroscopy (FTIR) was used to demonstrate the presence of the desired compounds and confirm an upright orientation on the gold substrates. The formation of appropriately hydrogen-bonded complexes on these surfaces was confirmed with surface plasmon resonance studies of the binding of hydrogen-bonded targets, and also with studies of the adhesion of functionalized atomic force microscope (AFM) probes.

B. Tip preparation and functionalization

STM tips were made from 0.25 mm diameter gold wire (purity 99.999% from Alfa Aesar) by either AC (30V, 4.2 KHz) or DC (2V) electrochemical etching in mixed solutions of concentrated HCl and ethanol (50:50, v/v). The gold tips were immersed in Piranha Solution (3:1 H_2SO_4:H_2O_2 - 30% by volume – use caution as this solution is extremely reactive and will explode on contact with organics for 30 s, rinsed with DI water and dried in an N_2 stream prior to use or modification. A typical procedure for functionalization is as follows: tips were immersed in a solution of the probe molecules for periods ranging from 2 hours to overnight, then rinsed with clean solvent repeatedly and blown dry in an N_2 stream. Tips for measurements in aqueous solution were coated with wax[46] or high density polyethylene.[49] High density polyethylene coatings are required when the tip functionalization procedure uses a solvent that dissolves wax insulation. We know of no analytical method sensitive enough to test for successful functionalization of the probes, so tunneling measurements are first carried out with unfunctionalized probes to provide a bench mark for recognizing unsuccessful funtionalization. We currently succeed in functionalizing the majority of the probes we prepare.

C. STM experiments

Measurements were carried out on a PicoSPM (Agilent, Chandler). The STM tip movement was controlled by custom labview programs and the data were recorded by a Yokogawa digital oscilloscope. 1,2,4-trichlorobenzene (TCB) and aqueous buffered electrolytes solution (0.1x PBS) were both used as working solutions. We performed i-z (STM break-junction) and i-t experiments (STM fixed junction) measurements. For i-z measurements, tunneling current (i) at fixed bias was recorded versus distance (z) while withdrawing tip from the surface in z direction.[10]

For i-t measurement, tunneling current (i) at fixed bias was recorded versus time (t) while holding tip at a fixed distance above the surface. We developed two methods for these “fixed gap” measurements: 1. Open loop without servo control.[15] 2. Closed loop with weak servo control.[19] For the open loop method, the junction is repeatedly reset by making ever smaller steps in the PZT voltage to avoid PZT creep. The junctions are found to be stable (no detectable shift in the background current) over periods of several seconds, perhaps as a result of the bonding process discussed above.

For the “closed loop” method, the STM servo gains were set low so that only spikes of long duration were affected by the action of the current-control servo. We characterized the response time of the servo by recording thermal noise spectra with, and without servo control.[19] The closed-loop method does cause some distortion in signals from bound states of long duration, but it is much easier to implement.

References

1. Hamers RJ, Tromp RM, Demuth JE. Surface Electronic Structure of Si (111)-(7×7) Resolved in Real Space. Phys. Rev. Lett 1986;56:1972–1975. [PubMed: 10032824]
2. Hipps, KW. Handbook of Applied Solid State Spectroscopy. Kluwer; Berlin: 2005. Scanning Tunneling Spectroscopy. in press
3. Shapir E, Cohen H, Calzolari A, Cavazzoni C, Ryndyk DA, Cuniberti G, Kotlyar A, Felice RD, Porath D. Electronic structure of single DNA molecules resolved by transverse scanning tunnelling spectroscopy. Nature Materials 2008;7:68–74.
4. Tanaka H, Kawai T. Partial sequencing of a single DNA molecule with a scanning tunnelling microscope. Nature Nanotechnology 2009;4:518–522.
5. Kuznetsov, AM.; Ulstrup, J. Electron transfer in chemistry and biology. Wiley; New York: 1999.

6. Cui XD, Primak A, Zarate X, Tomfohr J, Sankey OF, Moore AL, Moore TA, Gust D, Harris G, Lindsay SM. Reproducible measurement of single-molecule conductivity. Science 2001;294:571–574. [PubMed: 11641492]
7. Lindsay SM, Ratner MA. Molecular Transport Junctions: Clearing Mists. Advanced Materials 2007;19:23–31.
8. Tao N. Probing potential-tuned resonant tunneling through redox molecules with scanning tunneling microscopy. Phys. Rev. Letts 1996;76:4066–4069. [PubMed: 10061183]
9. Ohshiro T, Umezawa Y. Complementary base-pair-facilitated electron tunneling for electrically pinpointing complementary nucleobases. Proc. Nat. Acad. Sci 2006;103:10–14. [PubMed: 16373509]
10. Chang S, He J, Kibel A, Lee M, Sankey OF, Zhang P, Lindsay SM. Tunneling readout of hydrogen-bonding based recognition. Nature Nanotechnology 2009;4:297–301.
11. Frisbie CD, Rozsnyai F, Noy A, Wrighton MS, Lieber CM. Functional group imaging by chemical force microscopy. Science 1994;265:2071–4. [PubMed: 17811409]
12. Hinterdorfer P, Baumgartner W, Gruber HJ, Schilcher K, Schindler H. Detection and localization of individual antibody-antigen recognition events by atomic force microscopy. Proc. Natl. Acad. Sci. (USA) 1996;93:3477–3481. [PubMed: 8622961]
13. He J, Lin L, Zhang P, Lindsay SM. Identification of DNA base-pairing via tunnel-current ecay. Nano Letters 2007;7:3854–3858. [PubMed: 18041859]
14. He J, Lin L, Liu H, Zhang P, Fu Q, Lee M, Sankey O, Lindsay S. A hydrogen-bonded electron-tunneling circuit reads base composition of unmodified DNA. Nanotechnology 2009;20:075102, 1–8. [PubMed: 19417406]
15. Chang S, He J, Lin L, Zhang P, Liang F, Young M, Huang S, Lindsay S. Tunnel conductance of Watson-Crick nucleoside-basepairs from telegraph noise. Nanotechnology 2009;20:075102–075110. [PubMed: 19417406]
16. Ramachandran GK, Hopson TJ, Rawlett AM, Nagahara LA, Primak A, Lindsay SM. A Bond-Fluctuation Mechanism for Stochastic Switching in Wired Molecules. Science 2003;300:1413–1415. [PubMed: 12775835]
17. Haiss W, Nichols RJ, Zalinge H.v. Higgins SJ, Bethell D, Schiffrin DJ. Measurement of single molecule conductivity using the spontaneous formation of molecular wires. Phys. Chem. Chem. Phys 2004;6:4330–4337.
18. Haiss W, Wang C, Grace I, Batsanov AS, Schiffrin DJ, Higgins SJ, Bryce MR, Lambert CJ, Nichols RJ. Precision control of single-molecule electrical junctions. Nature Materials 2006;5:995–1002.
19. Chang S, Huang S, He J, Liang F, Zhang P, Li S, Chen X, Sankey OF, Lindsay SM. Electronic Signature of all four DNA Nucleosides in a Tunneling Gap. Nano Letters 2010;10:1070–1075. [PubMed: 20141183]
20. Datta, S. Electronic transport in mesoscopic systems. Cambridge University Press; Cambridge: 1990.
21. Datta, S. Quantum Transport: Atom to Transistor. Cambridge Univeristy Press; 2005.
22. Moth-Poulsen K, Bjørnholm T. Molecular electronics with single molecules in solid-state devices. Nature Nanotechnology 2009;4:551–556.
23. Mujica V, Kemp M, Ratner MA. Electron conduction in molecular wires. I. A scattering formalism. J. Chem. Phys 1994;101:6849–6855.
24. Nitzan A, Ratner M. Electron Transport in Molecular Wire Junctions. Since 2003;300:1384–1389.
25. Büttiker M. Four-terminal phase-coherent conductance. Phys. Rev. Lett 1986;57:1761–1764. [PubMed: 10033538]
26. Caroli C, Combescot R, Noziéres P, Saint-James D. Direct calculation of the tunneling current. J. Phys. C: Condensed Matter 1971;4:916.
27. Tomfohr JK, Sankey OF. Theoretical analysis of electron transport through organic molecules. J. Chem. Phys 2004;120:1542– 15554. [PubMed: 15268281]
28. Keldysh VL. Sov. Phys. JETP 1965;20:1018.
29. Brandbyge M, Mozos JL, Ordejon P, Taylor J, Stokbro K. Density-functional method for nonequilibrium electron transport. Phys. Rev. B 2002;65:165401.
30. Xue YQ, Datta S, Ratner MA. First-principles based matrix Green's function approach to molecular electronic devices: general formalism. Chemical Physics 2002;281:151–170.

31. Lindsay, SM. Introduction to Nanoscience. Oxford University Press; Oxford: 2009.
32. Chen F, He J, Nuckolls C, Roberts T, Klare J, Lindsay SM. A molecular switch based on potential-induced changes of oxidation state. Nano Letters 2005;5:503–506. [PubMed: 15755102]
33. Jeffrey, GA. An Introduction to Hydrogen Bonding. Oxford University Press; Oxford: 1997.
34. Tomfohr J, Sankey OF. Complex bandstructure, decay lengths and Fermi level alignment in simple molecular electronic systems. Phys. Rev. B 2002;65:245105–245105-12.
35. Lee, M. PhD in *Physics*.. Arizona State University; Tempe: 2009. Electronic Structure Simulations of DNA base recognition and Vibrational Property Analysis of Polyanionic Hydrides; p. 178
36. de Rege PJF, Williams SA, Therien MJ. Direct evaluation of electronic coupling mediated by hydrogen bonds: Implications for biological electron transfer. Science 1995;269:1409–1413. [PubMed: 7660123]
37. Lee MH, Sankey OF. Theory of tunneling across hydrogen-bonded base pairs for DNA recognition and sequencing. Phys. Rev .E 2009;79:051911, 1–10.
38. Xu B, Tao NJ. Measurement of Single-Molecule Resistance by Repeated Formation of Molecular Junctions. Science 2003;301:1221–1223. [PubMed: 12947193]
39. Venkataraman L, Klare JE, Tam IW, Nuckolls C, Hybertsen MS, Steigerwald ML. Single-Molecule Circuits with Well-Defined Molecular Conductance. Nano Lett 2006;6:458–462. [PubMed: 16522042]
40. Kresse G, Furthmuller J. Efficient iterative schemes for ab initio total-energy calculations using a plane-wave basis set. Phys. Rev. B 1996;55:11169–11186.
41. Perdew JP, Wang Y. Accurate and simple analytic representation of the electron-gas correlation energy. Phys. Rev. B 1992;45:13244.
42. Blanco JM, Flores F, Perez R. STM-theory: Image potential, chemistry and surface relaxation. Prog. Surf. Sci 2006;81:403.
43. Jelinek P, Wang H, Lewis JP, Sankey OF, Ortega J. Multicenter approach to the exchange-correlation interactions in ab initio tight-binding methods. Phys. Rev .B 2005;71:235101.
44. Jelinek P, Perez R, Ortega J, Flores F. Mechanical properties and electrical conductance of different Al nanowires submitted to an homogeneous deformation: a first-principles simulation. Surf. Sci 2004;566-568:1–13.
45. Rzeznicka II, Lee J, Maksymovych P, Yates JT. Nondissociative Chemisorption of Short Chain Alkanethiols on Au(111). J. Phys. Chem. B 2005;109:15992–15996. [PubMed: 16853029]
46. Nagahara LA, Thundat T, Lindsay SM. Preparation and Characterization of STM Tips for Electrochemical Studies. Rev. Sci. Instrum 1989;60:3128–3130.
47. Ehrlich M, Ehrlich K, Mayo JA. Unusual properties of the DNA from Xanthomonus phage p12 in which 5-methylcytosine copletely replaces cytosine. Biochimica et Biophysica Acta 1975;395:109–119. [PubMed: 1138935]
48. DeRose JA, Thundat T, Nagahara LA, Lindsay SM. Gold Grown Epitaxially on Mica: Conditions for Large Area Flat Faces. Surf. Sci 1991;256:102–108.
49. Visoly-Fisher I, Daie K, Terazono Y, Herrero C, Fungo F, Otero L, Durantini E, Silber J, Sereno L, Gust D, Moore TA, Moore AL, Lindsay SM. Conductance of a biomolecular wire. Proc. Nat. Acad. Sci 2006;103:8686–8690. [PubMed: 16728508]

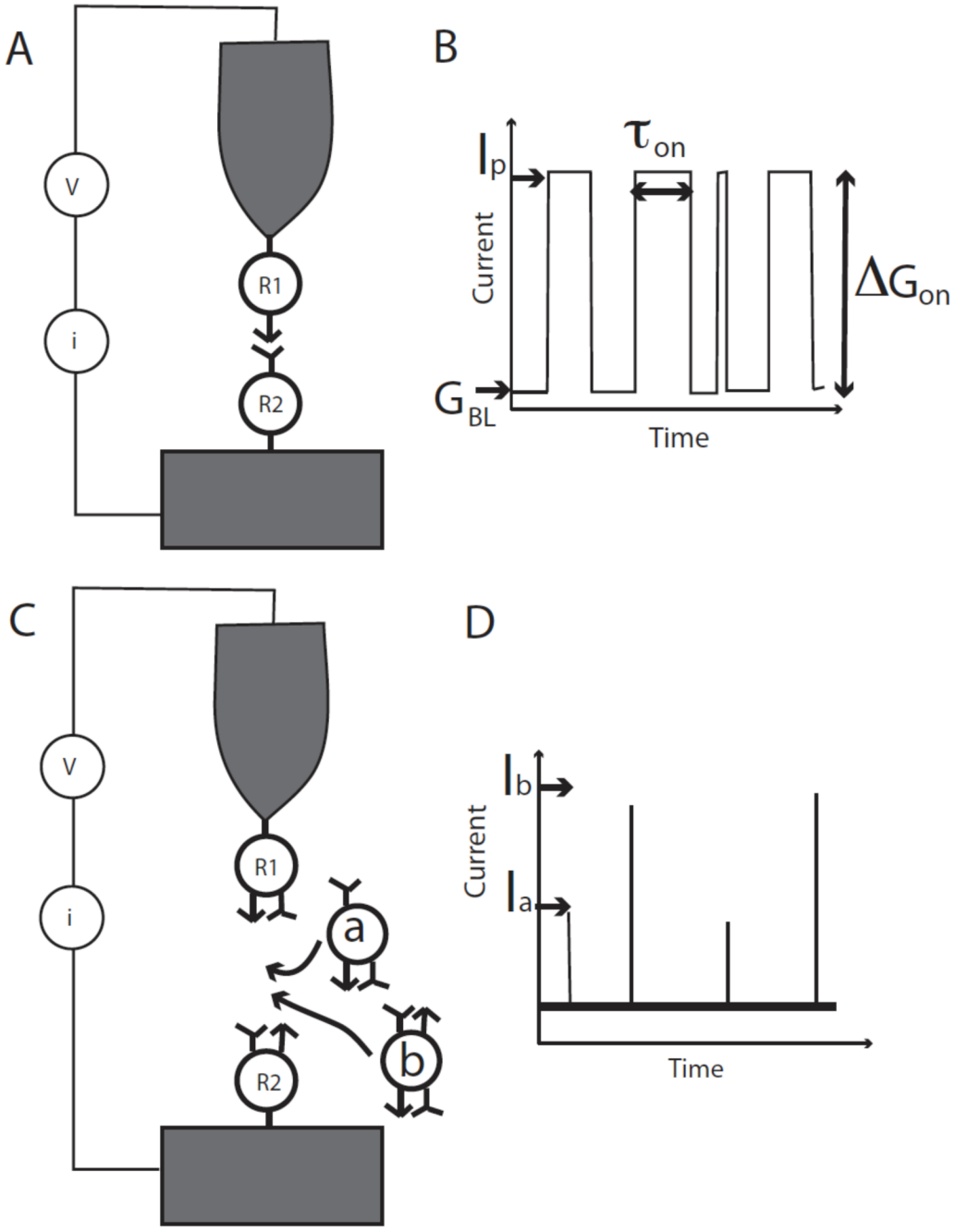

Figure 1.

Two configurations for Recognition Tunneling. In (A), the tethered molecule-pair junction, the current is recorded as a probe functionalized with a first recognition reagent (R1) is held above a surface functionalized with its bonding partner (R2). (B) Current recorded as a function of time shows switching fluctuations ("telegraph noise") as the junction between R1 and R2 breaks and remakes. The size of the gap is measured by the "open state current" I_0, which corresponds to a baseline conductance for the junction given by $G_{BL} = I_0/V$ where V is the junction bias. The change in conductance when the molecule binds to yield a peak conductance ($G_p = I_P/V$), $\Delta G_{ON} = G_P - G_{BL}$, is a measure of the conductance of a single molecule pair. The lifetime of the "bound" state can be measured using the width of the individual jumps in current

(τ). A second experimental configuration, the free-analyte configuration, is shown in (B). Here each electrode is functionalized with a reagent that presents recognition sites to a target (R1 and R2, but they could be the same reagent, for example one that presents a hydrogen bond donor and a hydrogen bond acceptor). The tunnel gap is set to a large value such that R1 and R2 do not interact with one another directly. Entry of an analyte into the gap ("a" or "b") causes a bonded pathway to be formed across the junction, leading to a "spike" in current through the junction (D). If the electron transmission of "a" and "b" differ significantly, their identity can be read directly from the size of the current spikes that are generated (Ia and Ib).

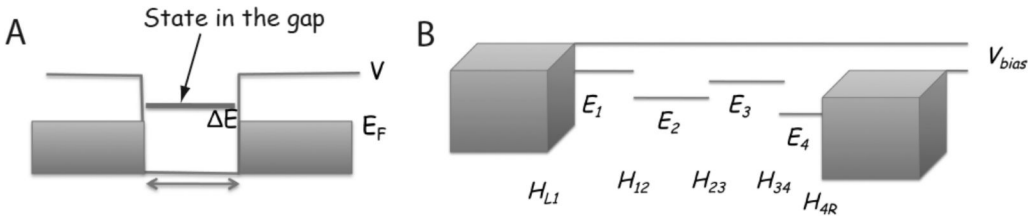

Figure 2.

Factors that control the tunneling signal: (A) A simple tunnel barrier shown as a 1D structure with a gap where the potential (V) exceeds the Fermi energy (E_F). This potential barrier, V-E_F, can be lowered to a value ΔE by the presence of an atom in the gap with an eigenstate at E_F+ΔE. The extension of this picture to a molecule in the gap is shown in (B) where each atom contributes a level near the gap E1, E2 .... and overlap between the atomic states (Hmn) leads to a delocalized state that connects the left and right electrodes. This mediates a current proportional to the number of available states on the positive electrode (i.e., proportional to V_{bias}) and the strength of the coupling between the electrodes, as given by the Green's function propagator.

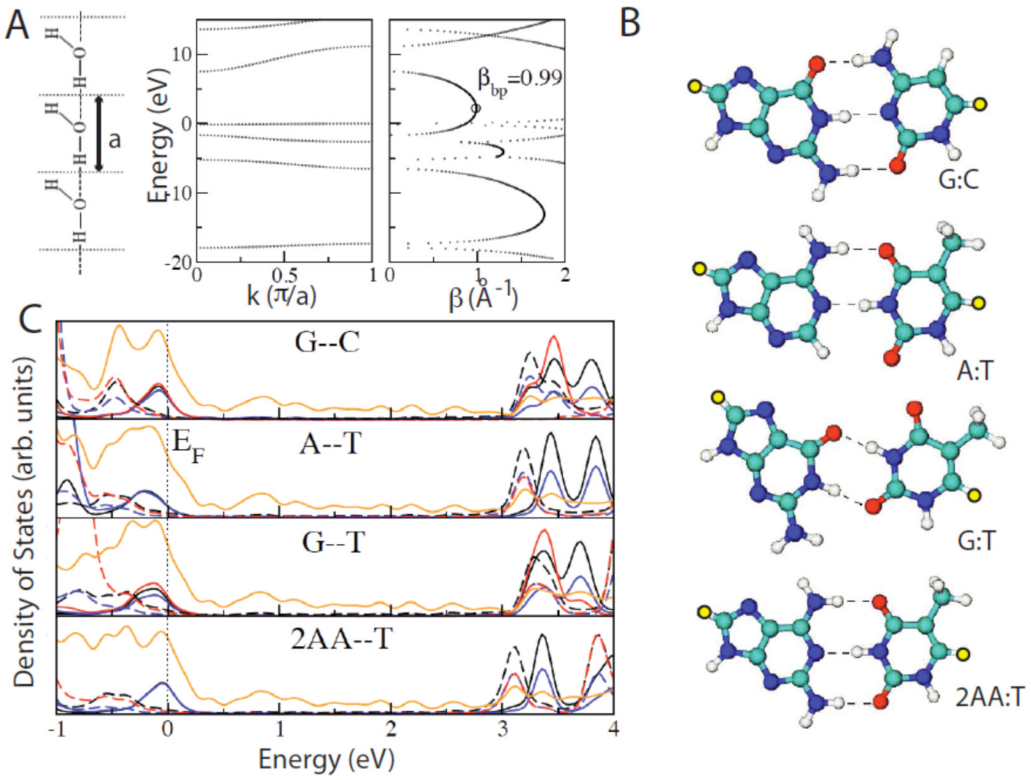

Figure 3.

Hydrogen-bond mediated tunneling. (A) A linear water chain model with one water molecule per unit cell. The H-O·····H angle is 180° and the O····H distance is 0.197 nm (left). The panels on the right show the allowed (real k) and gap (imaginary k or real β) states calculated using complex band structure. (B) Energy minimized configurations for the two Watson-Crick base pairs (G:C, A:T) a GT wobble base pare and a 2-aminoadenine:thymine (2AA:T) pair. Yellow atoms are sulfur atoms that connect to gold slabs. (C) Averaged projected densities of states (DOS) per atom for G--C, A--T, G--T, and 2AA--T base-pairs. The Fermi energy is defined to be zero energy. The projected DOS onto carbon, nitrogen, oxygen, and sulfur atoms are represented in black, blue, red, and orange colors. Solid and broken lines are the projected DOS onto atoms on purines (G, A, 2AA) and pyrimidines (C, T), respectively. The HOMO is dominated by the orbitals on purines (guanine for G-- C and G--T, adenine for A--T, and 2AA for 2AA--T) and the LUMO is dominated by the orbitals on pyrimidines (cytosine for G--C, thymine for G--T, A--T and 2AA--T).

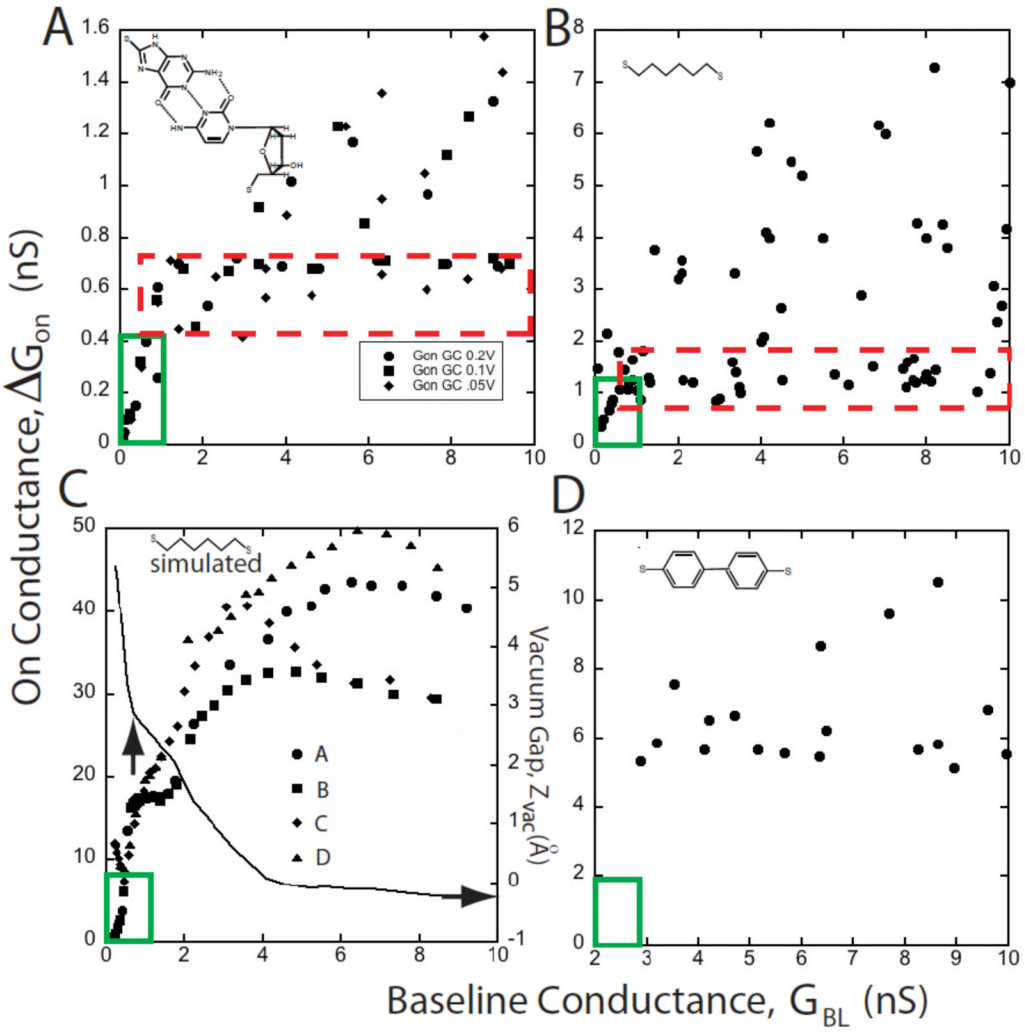

Figure 4.

Interpretation of scatter plots of the molecular conductance (ΔG_{ON}) vs. the baseline conductance (G_{BL}). (A) shows typical experimental data for a probe functionalized with a base (guanine) interacting with a surface-bound nucleoside (deoxycytidine). The red dashed box encloses a "plateau" region where the majority of the data are relatively constant. As G_{BL} is increased, the number of large conductance points also increases as do the largest values of ΔG_{ON}. At the smallest values of G_{BL} there is a region (solid green box) where $\Delta G_{ON} \propto G_{BL}$ and the data are single valued. Data for octanedithol show the same general features (B). Simulations for octanedithiol (C) reproduce these features. This plot was generated for a series of different contact geometries (A-D, illustrated in figure 5). The scatter increases as G_{BL} is increased in a way that closely resembles the experimental data in (B) (though calculated conductances are higher than the measured conductances). The simulations all converge at small G_{BL}, giving rise to a region where data are single valued and $\Delta G_{ON} \propto G_{BL}$, as observed in the experiments. The "plateau region" is less densely occupied in the simulated data, probably because of the limited number of tip geometries explored. In reality, we would expect to find many points around the periphery of the point forming the smallest gap that can accommodate molecules in their equilibrium configuration. The solid line in (C) shows the variation in the gap between the gold atom attached to the sulfur atom and the rest of the gold electrode (Z_{vac}). A nominal contact point (vertical arrow) is defined by the baseline conductance at which the slope of the Z_{vac} curve changes abruptly. This is coincident with the

transition from contact-independent conductance to contact dependent conductance. (D) shows data for a dithiol-diphenol. This “stiff” molecule yields no data in the $\Delta G_{ON} \propto G_{BL}$ regime, presumably because “stretched” configurations are not energetically possible in this molecule.

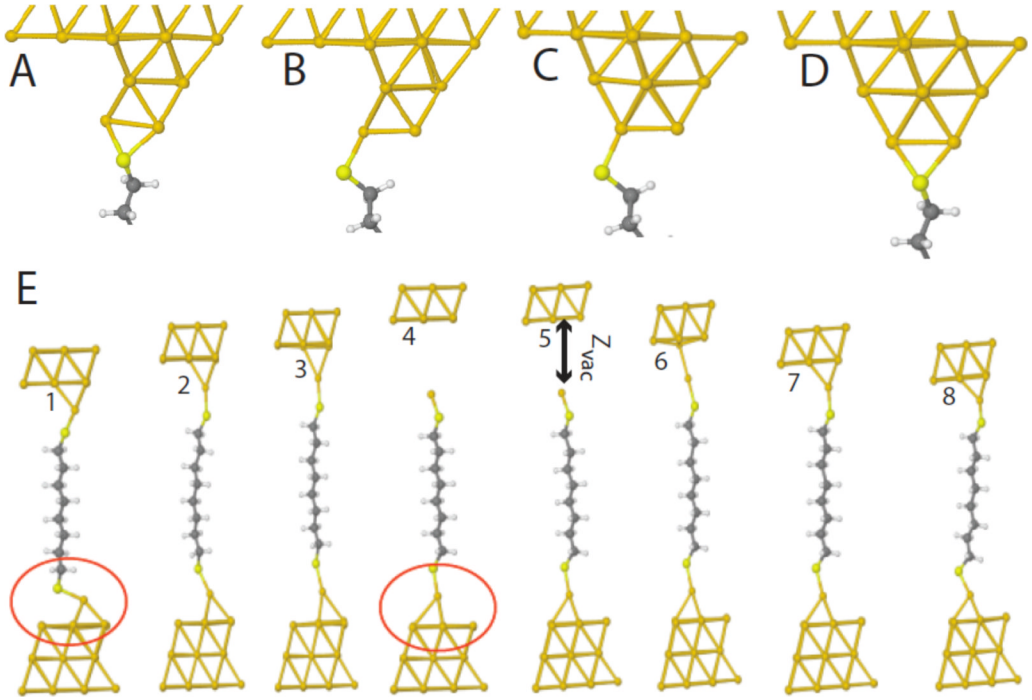

Figure 5.

Contact gepmetries. A-D show contacts of nearly equivalent energy for which the ΔG_{ON} vs. G_{BL} curves in Figure 4 were calculated. E1-E8 demonstrate an intrinsic instability in the surface bonding as a function of the tunnel gap size (note the differences between the two configurations circled in red). Note also how the molecule remains "stretched" (4,5 relative to 1,8) even after the bond to the electrode is "broken", a configuration that is presumably not available to stiffer molecules.

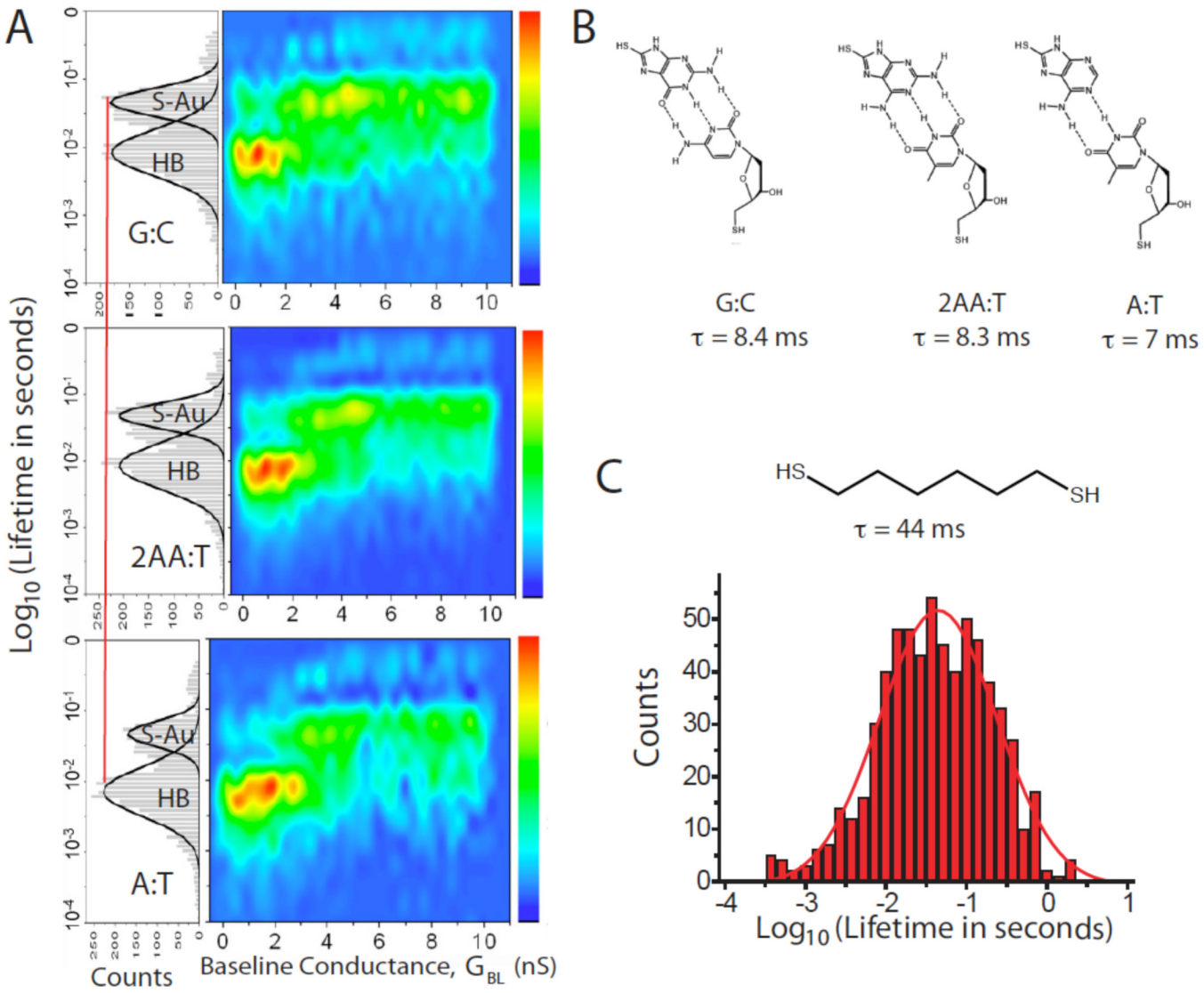

Figure 6.

Lifetime distributions from telegraph noise. (A) shows (left) distributions of the "on" state times for three types of DNA base-pairing (B) in a tunnel gap. Two peaks are observed in the distribution. One is a slower process that coincides with the peak that is observed in junctions with only (S-Au)-Au as the labile bonds (see the data for octane dithiol shown in (C)). The faster process is somewhat dependent on the nature of the hydrogen bonding, and is relatively more important in the A:T junctions (two hydrogen bonds) than the 2AA:T and G:C junctions (three hydrogen bonds). The distributions are broken out as a function of baseline conductance in the color plots to the right. Hydrogen bond-breaking is more important in the large gap (small G_{BL}) regime where the molecule is presumably stretched. (S-Au)-Au breaking dominates in smaller gaps.

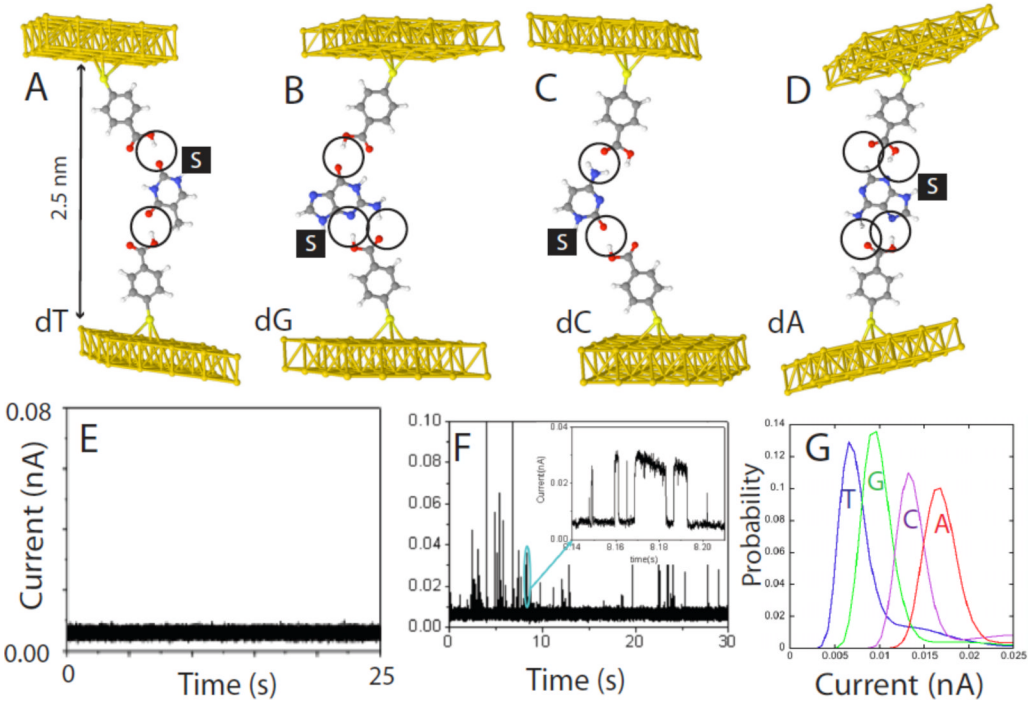

Figure 7.

"Free-analyte" configuration of Recognition Tunneling for reading DNA bases. (A-D) show energy-minimized structures for the four nucleosides bound in a 2.5 nm gap with 4-mercapto benzoic acid as the reading reagent (R1, R2 in Figure 1C). The "S" stands for the deoxyribose sugar (not shown) and the order (dT, dG, dC, dA) corresponds to the predicted order of increasing tunnel conductance using density functional theory. (E) Shows the background tunnel current in organic solvent (trichlorobenzene) with the gap set to G_{BL} = 12 pS (6pA at 0.5V bias). At this gap there is no indication of interactions between the two benzoic acid readers. (F) Shows an example of the current spikes that are observed when a solution of dG is injected into the tunnel junction. The inset shows details of some of the spike on a ms-timescale. Many of them show the telegraph noise switching characteristic of single molecule binding (the slight slope in the "on" level reflects the action of the servo used to control the tunnel gap). (G) Measured distributions of current for the four bases. The order agrees with the density-functional prediction, but the measured currents are larger than predicted. The overlap between reads limits the probability of a correct assignment on a single read to about 60%.

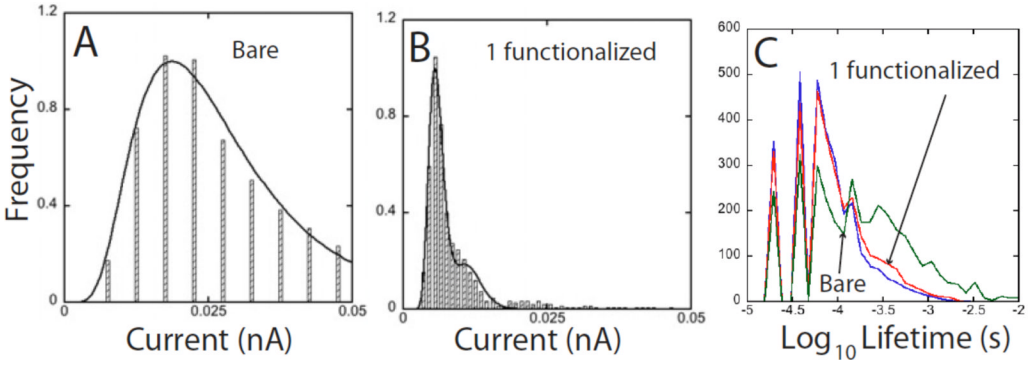

Figure 8.

Current distributions and binding modes: (A) Shows the current distribution measured for a pair of bare gold electrodes for dG. G_{BL} was increased to 20 pS to obtain these reads. (B) Shows the current distribution for dG with just one electrode functionalized. (C) Shows the distribution of on-state lifetimes for bare electrodes (blue), one electrode functionalized (red) and both electrodes functionalized (green). The fine structure reflects data binning. The three distributions are similar, implying that the narrowing that occurs on functionalizing one electrode comes from a smaller range of bound configurations in the gap and not a slowing of DNA motion.